



Synthesis, Characterization and Photocatalysis of Mesoporous TiO₂†

XIANGCHAO ZHANG^{1,2}, YANRONG JIA², QUMIN YU¹, AIDONG TANG² and SHIYING ZHANG^{1,*}

¹Key Laboratory of Application Technology of Environmental Photocatalysis of Hunan Province, Changsha University, Changsha 410003, Hunan Province, P.R. China

²School of Chemistry and Chemical Engineering, Central South University, Changsha 410083, Hunan Province, P.R. China

*Corresponding author: Fax: +86 731 84261440; Tel: +86 731 84261208; E-mail: cdzhangshiyang@163.com

AJC-15729

The mesoporous TiO₂ nanoparticulate has been prepared by evaporation induced self-assembly method using EO-PO type polyether P123 as a template. The small angle X-ray diffraction, wide angle X-ray diffraction, high-resolution transmission electron microscopy and N₂ isothermal adsorption-desorption are used to study the microstructure and morphology of the as-synthesized mesoporous TiO₂. The results demonstrate that the mesoporous TiO₂ belongs to anatase and the size is 20-30 nm. The sample is prepared using P123 as a template with average pore size distribution of 11.54 nm, specific surface area of 84.83 m²/g and pore volume of 0.234 cm³/g. The as-synthesized mesoporous TiO₂ exhibits remarkably high photocatalytic activity of 93.6 % in decomposing formaldehyde under ultraviolet light irradiations for 90 min. This work provides a basic experimental process for the preparation of mesoporous TiO₂, which will possess a broad prospect in terms of the applications in improving indoor air quality.

Keywords: Mesoporous TiO₂, Evaporation induced self-assembly, Photocatalysis, Formaldehyde.

INTRODUCTION

Because of the increasingly serious energy and environmental challenges, the sustainable and clean solar energy has been extensively exploited in recent years^{1,2}. Among existing approaches, photocatalysis is a promising method in the effective use of solar energy due to the significant advantages of efficient, stable and environmentally-friendly³⁻⁵. Since Fujishima and Honda⁶ first discovered the photolysis of water on TiO₂, TiO₂ has been widely used in water splitting⁷, water purification⁸ and carbon dioxide conversion⁹ because of its advantages such as low cost, good high photocatalytic activity, chemical stability and nontoxic nature¹⁰⁻¹². Considering that the effective use of solar energy, much effort have been spent in developing visible-light-driven TiO₂ photocatalysts such as dye-sensitization, non-metal doping and metal-ion doping. However, organic dyes are instability on light irradiation¹³ and metal ions act as the recombination centers of photoelectrons and holes in the photocatalytic performance¹⁴, which extremely reduces its photocatalytic activity that is determined by different factors such as the migration distance of charges, reactive sites and the number of defects. From the above point of view, it is necessary to prepare photocatalysts with the large surface area and high crystallinity.

Recently, mesoporous TiO₂ has attracted considerable attention because of its large surface area to offer more reactive sites. Antonelli first reported mesoporous titanium dioxide (TiO₂) was synthesized by sol-gel method with amine surfactants as template¹⁵. Subsequently, many researchers explore different template agents, such as block polymer¹⁶, dodecyl amine¹⁷, ionic or non-ionic surfactants¹⁸. However, most of the above mentioned TiO₂ mesoporous materials with large surface area have an amorphous channel wall, which must be calcined at a higher temperature in order to obtain a crystalline anatase phase. Although it causes a collapse of mesopores in the process of calcination and leads to a marked decrease in surface area^{19,20}. Therefore, It is indispensable to seek new methods for the synthesis of mesoporous TiO₂ with high photocatalytic activity.

In this paper, the mesoporous TiO₂ is synthesized by the evaporation induced self-assembly using EO-PO type polyether P123 as a template. The small angle X-ray diffraction (SARD), wide angle X-ray diffraction (WARD), high-resolution transmission electron microscopy (HR-TEM) and N₂ isothermal adsorption-desorption are used to study the microstructure and morphology of as-synthesized mesoporous TiO₂. The photocatalytic activity of as-synthesized mesoporous TiO₂

†Presented at 2014 Global Conference on Polymer and Composite Materials (PCM2014) held on 27-29 May 2014, Ningbo, P.R. China

for degradation of formaldehyde under UV light irradiations is also investigated.

EXPERIMENTAL

Preparation of mesoporous TiO₂ by evaporation induced self-assembly: The mesoporous TiO₂ was synthesized by the evaporation induced self-assembly using tetrabutyl titanate (Ti(OC₄H₉)₄, TTBO), acetylacetone (C₅H₈O₂, AcAc), anhydrous alcohol (C₂H₅OH, EtOH), EO-PO type polyether P123 and nitric acid (HNO₃, 65-68 %) as starting materials. All reagents were analytical grade and used without further purification. In this synthesis process, 17 mL tetrabutyl titanate was mixed with 5 mL acetyl acetone and 5 mL EtOH magnetically stirred for 0.5 h at room temperature, which was nominated as solution A. Solution B was prepared by mixing 2.0 g P123, 0.9 mL deionized water and 2.5 mL HNO₃ dissolving in 10 mL EtOH, add solution B to solution A (2 s/d) stirring vigorously for 2 h. In process of the stirring, the tetrabutyl titanate was hydrolyzed by the H₂O. The acetyl acetone and HNO₃ serve as the stabilizer to slow down the hydrolysis of tetrabutyl titanate. The transparent solids were left in glass plates (1-2 mm viscous liquid layers) at *t* = 60 °C. Translucent glasslike xerogels were obtained due to solvent evaporation. As-synthesized samples were undergone to mild thermal treatment (100 °C overnight) to enhance the inorganic network. The mesoporous TiO₂ was prepared after calcined at 450 °C for 3 h.

Characterization: The powder X-ray diffraction (XRD) patterns of as-synthesized mesoporous TiO₂ were determined using Bruker AXS D8 Advance X-ray diffractometer with CuK_α radiation ($\lambda = 0.15406$ nm) in the 2 θ range of 10-80°. The morphology of photocatalyst was characterized by high-resolution transmission electron microscopy (HR-TEM, JEM-3010) at an operating accelerating voltage of 200 kV with spot resolution of 0.19 nm. The pore size distribution and Brunauer-Emmett-Teller (BET) surface area of the mesoporous TiO₂ particles were determined by nitrogen adsorption-desorption isotherm measurements at 77 K on a Quantachrome Autosorb-1 analyzer. All the measured samples were degassed at 180 °C for 3 h before the measurement. Pore size distribution and pore volume were calculated by the Barrett-Joyner-Halenda (BJH) method using the Halsey equation.

Photocatalytic activity: The photocatalytic activity of the photocatalyst for degrading formaldehyde was based on Chinese standard of HJ601-2011 (acetylacetone spectrophotometric method). In a typical process, 100 mL of formaldehyde solution of concentration 10 mg/L was taken in the reactor along with 0.1 g catalyst and the mixture was irradiated under a 30 W ultraviolet light. Before illumination, the suspension was magnetically stirred for 0.5 h in the dark to reach an adsorption/desorption balance of formaldehyde on the catalyst surface. The formaldehyde concentration was measured with a UV-visible spectrophotometer, the maximum absorption peak of formaldehyde was at $\lambda = 414$ nm. The degrading rate *D* was calculated as follow:

$$D = \frac{(C_0 - C)}{C_0} \times 100 \%$$

*C*₀: the initial concentration of formaldehyde (mg/L); *C*: formaldehyde concentration at special time point (mg/L).

RESULTS AND DISCUSSION

The wide-angle XRD and small-angle XRD patterns of the synthesized mesoporous TiO₂ are provided in Fig. 1. As shown in Fig. 1a, The diffraction peaks of the sample can be readily indexed to diffraction peak of anatase phase TiO₂ (JCPDS 21-1272) for the samples, which clearly shows the presence of nanocrystalline anatase. Fig. 2b shows the sharp diffraction peak at 2 θ = 1.0-1.5°, which demonstrate that the well-organized mesostructure has been formed, which can be confirmed by the results of HR-TEM and nitrogen adsorption-desorption isotherm measurements.

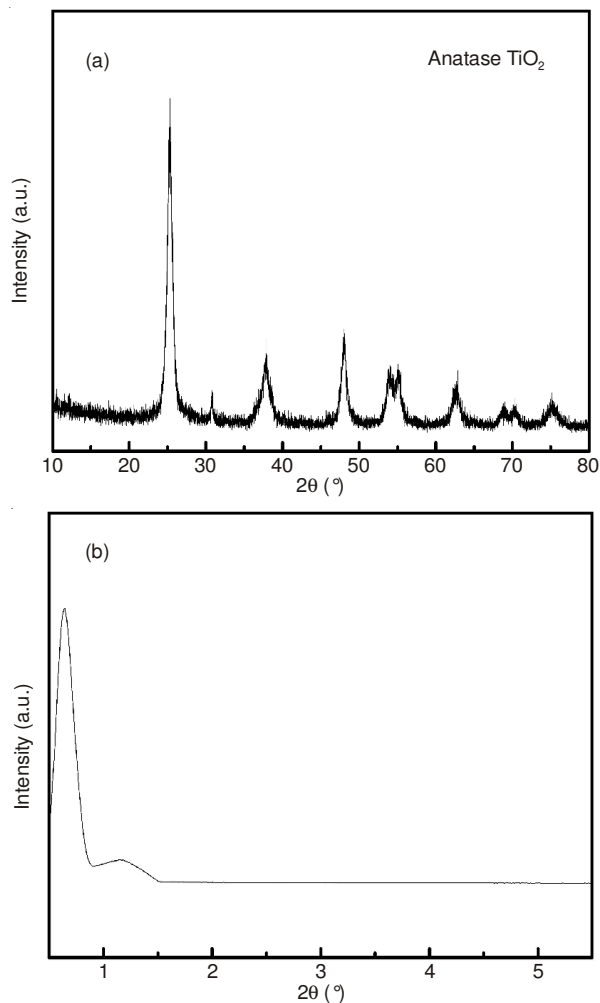


Fig. 1. XRD patterns of the synthesized mesoporous TiO₂: (a) wide-angle XRD; (b) small-angle XRD

HR-TEM results provide some information about the microstructure and morphology of the mesoporous TiO₂. Fig. 2 reveals a typical TEM image of the mesoporous TiO₂ calcined at 450 °C for 3 h, which demonstrates that the mesoporous TiO₂ particles are consisted of nanoparticles with the diameter in the range of 20-30 nm. The porous structure of the synthesized TiO₂ can also be seen, which is formed by the dense packing of nanoparticles. The grain boundary of sample is clearly observed, indicating that the nanoparticles have the very high crystallinity. The results of HRTEM demonstrate that the mesostructure TiO₂ is as well-organized as in the case of as-synthesized TiO₂.

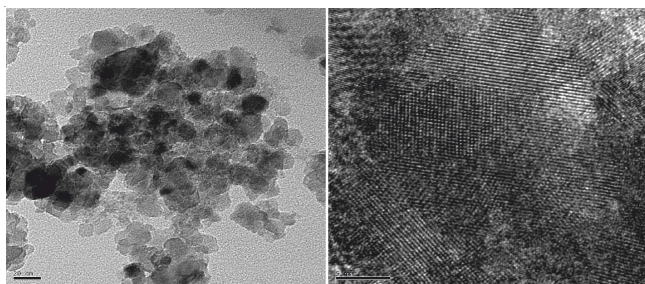


Fig. 2. HR-TEM images of the synthesized mesoporous TiO₂

The SEM images of the synthesized mesoporous TiO₂ are shown in Fig. 3. The as-obtained TiO₂ consists mainly of irregular agglomerated particles with the diameter in the range of 10-30 nm, which is consistent with the HR-TEM.

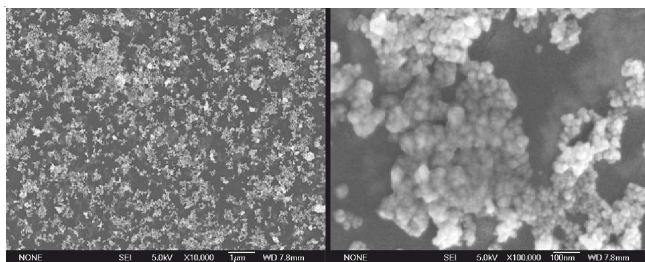


Fig. 3. SEM images of the synthesized mesoporous TiO₂

Fig. 4a shows the nitrogen adsorption-desorption isotherms of the sample and the corresponding Barret-Joyner-Halenda (BJH) pore size distributions plot (calculated from the adsorption branch) is presented in Fig. 4b. According to IUPAC classification²¹, the similar nitrogen adsorption-desorption isotherms of sample can be classified as Langmuir IV isotherm and the hysteresis loop is H2, which is typical of the mesoporous materials. The hysteresis loop at high relative pressure and the sharp decline in the desorption curve that indicate TiO₂ has the mesoporous structure. From Fig. 4b, it can be seen that the average pore sizes of mesostructure TiO₂ is about 11.54 nm. The shape of the curve, in agreement with results of small-angle XRD and HRTEM results, shows the absence of a narrow pore size distribution. The calculated BET specific surface area and pore volume are 84.83 m²/g and 0.234 cm³/g, respectively.

The degradation rates of formaldehyde over the as-prepared TiO₂ and Degussa P25 under UV light irradiation are shown in Fig. 5. It indicates that the photodegradation ratio of formaldehyde increases with the increase of photocatalytic time. The highest degradation rate of formaldehyde for the mesoporous TiO₂ is 93.6 % at 90 min, while that for Degussa P25 is only 65.5 %. The results show that the photocatalytic activity of formaldehyde degradation is better improved for the mesoporous TiO₂ than that for P25.

Conclusion

The mesoporous TiO₂ have been synthesized by evaporation induced self-assembly method. The as-synthesized mesoporous TiO₂ is anatase with the uniform size 20-30 nm, average pore size distribution of 11.54 nm, specific surface area of 84.83 m²/g and pore volume of 0.234 cm³/g, respectively. The sample shows higher catalytic performance than

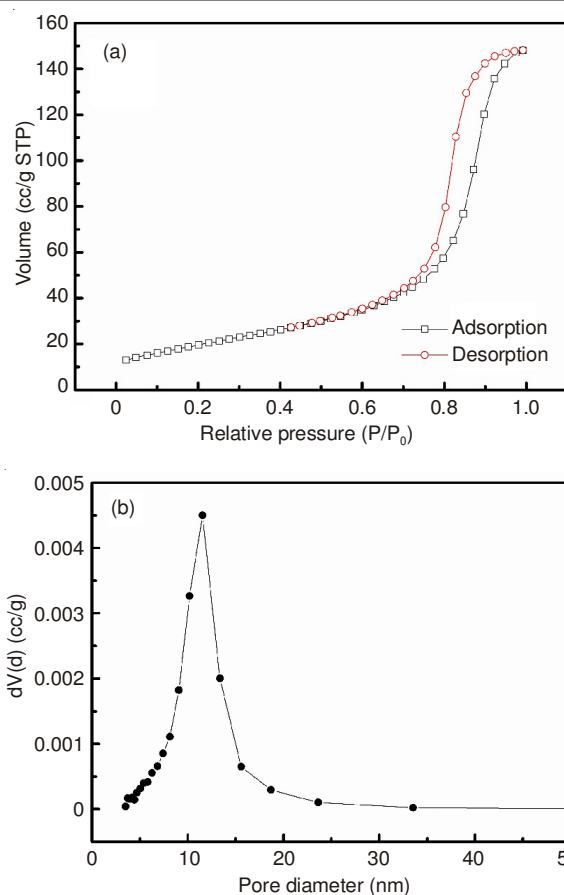


Fig. 4. Nitrogen adsorption-desorption isotherms (a) and Pore size distribution curve (b) of the synthesized mesoporous TiO₂

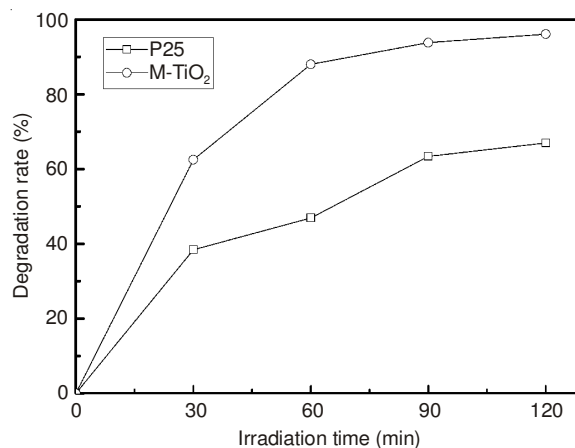


Fig. 5. Photocatalytic degradation rate of formaldehyde for the as-prepared mesoporous TiO₂ and Degussa P25, respectively

P25, in the presence of mesoporous TiO₂ decomposition of formaldehyde reached 93.6 % under ultraviolet light irradiations for 90 min.

ACKNOWLEDGEMENTS

This work was supported by the Program for the National Natural Science Foundation of China (51102026, 51272032) and Scientific Research Fund of Hunan Provincial Education Department(11A014) and Aid Program for Science and Technology Innovative Research Team in Higher Educational Institutions of Hunan Province.

REFERENCES

1. A. Kudo and Y. Miseki, *Chem. Soc. Rev.*, **38**, 253 (2008).
2. C. An, S. Peng and Y. Sun, *Adv. Mater.*, **22**, 2570 (2010).
3. Q. Zhang, J.-B. Joo, Z. Lu, M. Dahl, D.Q.L. Oliveira, M. Ye and Y. Yin, *Nano Res.*, **4**, 103 (2011).
4. M. Anpo, *Pure Appl. Chem.*, **72**, 1265 (2000).
5. Y.P. Liu, L. Fang, H.D. Lu, L.J. Liu, H. Wang and C.Z. Hu, *Catal. Commun.*, **17**, 200 (2012).
6. A. Fujishima and K. Honda, *Nature*, **238**, 37 (1972).
7. A.J. Cowan, J. Tang, W. Leng, J.R. Durrant and D.R. Klug, *J. Phys. Chem. C*, **114**, 4208 (2010).
8. H. Bai, Z. Liu and D.D. Sun, *Chem. Commun. (Camb.)*, **46**, 6542 (2010).
9. S.S. Tan, L. Zou and E. Hu, *Catal. Today*, **115**, 269 (2006).
10. J.Y. Shi, J. Chen, Z.C. Feng, T. Chen, Y.X. Lian, W.L. Wang and C. Li, *J. Phys. Chem. C*, **111**, 693 (2007).
11. J. Zhang, Q. Xu, Z.C. Feng, M.J. Li and C. Li, *Angew. Chem. Int. Ed.*, **47**, 1766 (2008).
12. J. Pan, G. Liu, G.Q. Lu and H.M. Cheng, *Angew. Chem. Int. Ed.*, **50**, 2133 (2011).
13. A.V. Emeline, V.N. Kuznetsov, V.K. Rybchuk and N. Serpone, *Int. J. Photoenergy*, Article ID 258394 (2008).
14. F.B. Li, X.Z. Li and M.F. Hou, *Appl. Catal. B*, **48**, 185 (2004).
15. D.M. Antonelli, *Micropor. Mesopor. Mater.*, **30**, 315 (1999).
16. B. Smarsly, D. Grosso, T. Brezesinski, N. Pinna, C. Boissière, M. Antonietti and C. Sanchez, *Chem. Mater.*, **16**, 2948 (2004).
17. T.V. Anuradha and S. Ranganathan, *Bull. Mater. Sci.*, **30**, 263 (2007).
18. G.Q. Liu, Z.G. Jin, X.X. Liu, T. Wang and Z.F. Liu, *J. Sol-Gel Sci. Technol.*, **41**, 49 (2007).
19. D. Chen, F. Huang, Y.B. Cheng and R.A. Caruso, *Adv. Mater.*, **21**, 2206 (2009).
20. C. Bai and M. Liu, *Angew. Chem. Int. Ed.*, **52**, 2678 (2013).
21. K.S.W. Sing, D.H. Everett, R.A.W. Haul, L. Moscou, R.A. Pierotti, J. Rouquerol and T. Siemieniowska, *Pure Appl. Chem.*, **57**, 603 (1985).